DOI: 10.1002/anie.201006357

Carbocations

IR Spectrum and Structure of the Phenyl Cation**

*Alexander Patzer, Shamik Chakraborty, Nicola Solcà, and Otto Dopfer**

The phenyl cation (c-$C_6H_5^+$, Figure 1) is a fundamental carbocation in aromatic hydrocarbon chemistry. It results from dehydrogenation of the benzene cation, the smallest member of the arene family. c-$C_6H_5^+$ is an ubiquitous ion in (extra-)terrestrial hydrocarbon plasmas[1] and mass spectra of aromatic molecules.[2] It is of importance to organic chemistry due to its extreme electrophilicity arising from the vacant nonbonding σ orbital (LUMO). Owing to its high reactivity, c-$C_6H_5^+$ has escaped so far spectroscopic characterization in the gas phase. Herein, we report the IR spectrum of isolated c-$C_6H_5^+$ obtained by Ar-tagging IR photodissociation (IRPD). This IRPD approach was previously used to elucidate the structure of related fundamental hydrocarbon ions, e.g., $C_6H_7^+$,[3] $C_2H_5^+$,[4] and $C_3H_3^+$.[5]

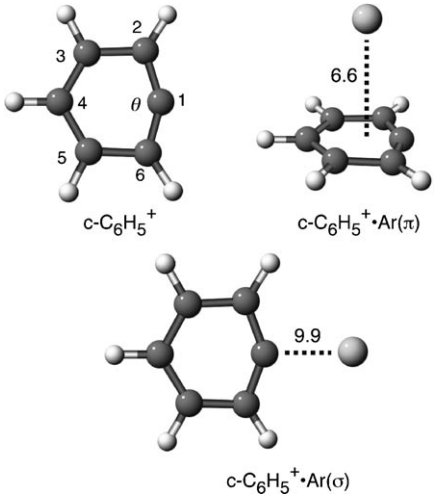

Figure 1. Structures and intermolecular binding energies (in kJ mol^{-1}) of c-$C_6H_5^+$ and the two most stable c-$C_6H_5^+$·Ar dimers calculated at the MP2/aug-cc-pVTZ level. Relevant structural parameters are listed in Table 1.

Quantum chemical calculations demonstrate that c-$C_6H_5^+$ has a planar structure with C_{2v} symmetry in its $^1A_1$ ground electronic state (Table 1).[6–8] Although never directly observed as a stable species in solution, c-$C_6H_5^+$ has been invoked as reactive intermediate in chemical reactions such as dediazoniation.[9] Recently, c-$C_6H_5^+$ was isolated in an Ar matrix by photolysis of halobenzenes and subsequent photoionization,[7] and IR spectroscopic identification was achieved through the observation of two intense vibrational transitions and isotopic labeling. Despite considerable efforts, spectroscopic characterization of the geometric and electronic structure of c-$C_6H_5^+$ in the gas phase is still lacking. Photoionization of c-C_6H_5 yields congested spectra[10] due to the large geometry change involved in ionization.[6b] Ion chemistry and mass spectrometric experiments[11–13] yield insight into the reactivity and relative stability of cyclic and acyclic $C_6H_5^+$ isomers (a-$C_6H_5^+$) but do not provide direct information about their structure.

Table 1: Selected bond lengths *R* (in Å) and angles (in degrees) of c-$C_6H_5^+$ and the most stable c-$C_6H_5^+$·Ar dimers calculated at the MP2/aug-cc-pVTZ level.

	c-$C_6H_5^+$	c-$C_6H_5^+$·Ar(σ)	c-$C_6H_5^+$·Ar(π)
$R_{C_1C_2}$	1.3196	1.3436	1.3193
$R_{C_2C_3}$	1.4379	1.4171	1.4376
$R_{C_3C_4}$	1.3908	1.3926	1.3907
R_{C_2H}	1.0790	1.0782	1.0791
R_{C_3H}	1.0838	1.0826	1.0839
R_{C_4H}	1.0805	1.0806	1.0806
∡C6-C1-C2 (θ)	149.6	140.2	149.6
∡C1-C2-C3	102.7	128.2	102.7
∡C2-C3-C4	122.0	121.5	122.0
∡C3-C4-C5	120.9	121.1	121.0

The sensitive technique of IRPD spectroscopy of mass-selected ions was used here to derive the IR spectrum of c-$C_6H_5^+$.[14] Weakly bound Ar atoms were attached to the ions to facilitate resonant single-photon fragmentation (Ar-tagging).[3,4,15] The IRPD spectra of $C_6H_5^+$·Ar in the CH stretch range shown in Figure 2 were obtained using two different precursors for generating $C_6H_5^+$, fluorobenzene (spectrum a in Figure 2), and benzaldehyde (spectrum b). Comparison of the two spectra reveals five bands in the 3000–3150 cm^{-1} range (A–E, Table 2), which occur in both spectra with the same relative intensities and are thus assigned to the five possible CH stretch fundamentals (σ_{CH}) of c-$C_6H_5^+$. Spectrum (a) displays additional intense features X–Z at 2970, 3200, and 3276 cm^{-1}, whose intensities are largely reduced in spectrum (b). They are attributed to a-$C_6H_5^+$·Ar dimers. The formation of less stable a-$C_6H_5^+$ isomers is largely suppressed using electron ionization of benzaldehyde rather than fluoroben-

[*] Dipl.-Phys. A. Patzer, Dr. S. Chakraborty, Dr. N. Solcà,[+]
Prof. Dr. O. Dopfer
Institut für Optik und Atomare Physik
Technische Universität Berlin
Hardenbergstrasse 36, 10623 Berlin (Germany)
Fax: (+49) 30-3142-3018
E-mail: dopfer@physik.tu-berlin.de

[+] Present address: Sezione Della Protezione Dell'Aria Dell'Acqua e Del Suolo, Via Salvioni 2a, 6500 Bellinzona (Switzerland)

[**] This study was supported by the Deutsche Forschungsgemeinschaft (DO 729/2 and 729/3) and the Fonds der Chemischen Industrie.

Supporting information for this article is available on the WWW under http://dx.doi.org/10.1002/anie.201006357.

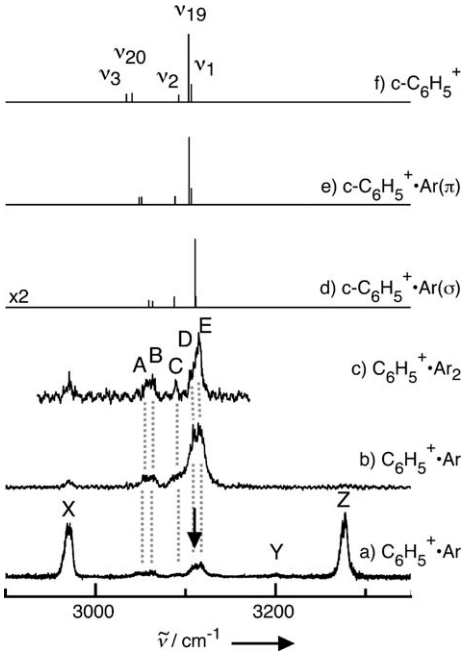

Figure 2. Experimental IRPD spectra of $C_6H_5^+$·Ar (a, b) and $C_6H_5^+$·Ar_2 (c) compared to linear stick IR absorption spectra of c-$C_6H_5^+$·Ar(σ) (d), c-$C_6H_5^+$·Ar(π) (e), and c-$C_6H_5^+$ (f) calculated at the MP2/aug-cc-pVTZ level. The intensities of the c-$C_6H_5^+$·Ar(σ) spectrum are multiplied by 2. IRPD spectra of $C_6H_5^+$·Ar are obtained using fluorobenzene (a) and benzaldehyde (b) as precursor. The positions and assignments of the transitions observed are listed in Table 2. Although the IRPD spectrum of $C_6H_5^+$·Ar was scanned in the 2710–3780 cm^{-1} range, transitions were only detected in the 2900–3350 cm^{-1} range shown here. The arrow indicates the position of the C–H stretch band observed in an Ar matrix (3110 cm^{-1}).[7]

Table 2: Positions of the transitions A–E (in cm^{-1}) observed in the IRPD spectra of $C_6H_5^+$·Ar_n compared to CH stretch frequencies (in cm^{-1}) of c-$C_6H_5^+$, c-$C_6H_5^+$·Ar(σ), and c-$C_6H_5^+$·Ar(π) calculated at the MP2/aug-cc-pVTZ level (Figure 2).[a]

	$\nu_3(a_1)$	$\nu_{20}(b_2)$	$\nu_2(a_1)$	$\nu_{19}(b_2)$	$\nu_1(a_1)$
c-$C_6H_5^+$	3034 (24)	3041 (27)	3092 (22)	3103 (211)	3106 (54)
c-$C_6H_5^+$·Ar(σ)	3059 (11)	3063 (9)	3087 (16)	3110 (106)	3112 (17)
c-$C_6H_5^+$·Ar(π)	3048 (22)	3051 (23)	3088 (26)	3104 (209)	3107 (50)
band	A	B	C	D	E
$C_6H_5^+$·Ar[b]	3055	3063	3090	3111	3117
$C_6H_5^+$·Ar[c]	3056	3063	3090	3110	3116
$C_6H_5^+$·Ar_2[c]	3057	3063	3089	3109	3115

[a] IR intensities in km mol^{-1} are listed in parentheses. Harmonic frequencies are scaled by 0.951. [b] Using fluorobenzene as precursor (Figure 2a). [c] Using benzaldehyde as precursor (Figure 2b).

zene. Hence, the IRPD spectrum of $C_6H_5^+$·Ar_2 (c) was obtained using benzaldehyde. It is similar in appearance to that of $C_6H_5^+$·Ar (b) but displays higher spectral resolution (5 vs. 10 cm^{-1}) due to the lower effective temperature of the larger cluster.

MP2/aug-cc-pVTZ calculations elucidate energetic, structural, and vibrational properties of c-$C_6H_5^+$·Ar_n (Figures 1 and 2, Tables 1 and 2). In line with previous results,[6–8] c-$C_6H_5^+$ has a planar equilibrium structure (C_{2v}) with alternating C–C bond lengths in its $^1A_1$ ground state. The rather different lengths of nonequivalent C–H bonds lead to largely decoupled σ_{CH} normal modes. The two relatively short *ortho* C–H bonds (R_{C_2H} =1.0790 Å) give rise to symmetric and antisymmetric σ_{CH} modes with high frequency, $\nu_1(a_1) = 3106$ and $\nu_{19}(b_2) = 3103$ cm^{-1}. The longer *para* C–H bond (R_{C_4H} =1.0805 Å) is associated with an isolated local σ_{CH} mode with lower frequency, $\nu_2(a_1) = 3022$ cm^{-1}. The weakest C–H bonds are in *meta* position and result in symmetric and antisymmetric σ_{CH} modes with the lowest frequencies, $\nu_3(a_1) =$ 3034 and $\nu_{20}(b_2) = 3041$ cm^{-1}. All σ_{CH} fundamentals are IR active with predicted intensities of 20–200 km mol^{-1}. Removal of H from the regular C_6H_6 hexagon implies substantial structural rearrangments, with the most significant change in the C2-C1-C6 bond angle θ, which opens up from 120° in C_6H_6 to 150° in c-$C_6H_5^+$. The vacant in-plane nonbonding σ orbital at C1 (LUMO) is very electrophilic ($q_{C1} = +0.67$ e) and attracts electron density from Ar and other nucleophilic ligands.[8,9,13,16]

Several minima were located on the c-$C_6H_5^+$·Ar potential. The global minimum corresponds to the planar c-$C_6H_5^+$·Ar(σ) structure (C_{2v}, Figure 1). The short intermolecular C1–Ar bond (2.2 Å) is characterized by a binding energy of $D_0 =$ 9.9 kJ mol^{-1} and an intermolecular stretch frequency of $\nu_s =$ 88 cm^{-1}. Ar donates electron density (0.23 e) into the electrophilic σ orbital of c-$C_6H_5^+$ upon formation of the weak chemical C–Ar bond. This situation is qualitatively similar to CH_3^+·Ar, where even larger charge transfer causes a much stronger C–Ar bond (ca. 0.5 eV),[17,18] demonstrating that the vacant $2p_z$ orbital of CH_3^+ is more electrophilic than the σ orbital of c-$C_6H_5^+$. As a result of the charge transfer, θ contracts from 150° to 140° in c-$C_6H_5^+$·Ar(σ) and the C–C bond length alternation becomes less pronounced. Also, the C–H bond lengths, σ_{CH} frequencies, and IR intensities are slightly affected. The small contraction of the C2–H bond (0.0008 Å) translates into an increase in ν_1 and ν_{19} by 6–7 cm^{-1}. The larger contraction of the C3–H bond (0.0012 Å) increases ν_3 and ν_{20} by 22–25 cm^{-1}, while R_{C_4H} and ν_2 are nearly unaffected upon Ar complexation. The charge transfer in c-$C_6H_5^+$·Ar(σ) reduces the IR intensities of all σ_{CH} fundamentals by a factor of 2–3.

The π-bonded c-$C_6H_5^+$·Ar isomer with C_s symmetry, c-$C_6H_5^+$·Ar(π), is considerably less stable than c-$C_6H_5^+$·Ar(σ). The π bond is based on dispersion and induction forces, and characterized by $D_0 = 6.6$ kJ mol^{-1}, an Ar–ring separation of 3.32 Å, and $\nu_s = 66$ cm^{-1}. The latter values are typical for π complexes of aromatic ions with Ar.[3,19,20] The weak π bond has nearly no effect on the geometry of c-$C_6H_5^+$, with changes in bond lengths and angles of < 0.0001 Å and < 0.1°. Hence, the σ_{CH} frequency shifts are < 15 cm^{-1} (0.5 %) and IR intensities are nearly unchanged. There are two further local minima on the c-$C_6H_5^+$·Ar potential with bond energies of 5.4 and 4.6 kJ mol^{-1}, respectively.[21]

The IRPD spectrum of $C_6H_5^+\cdot Ar$ in the σ_{CH} range closely resembles the spectrum predicted for c-$C_6H_5^+\cdot Ar(\sigma)$. Thus, bands A–F are assigned to this isomer, which is the global minimum on the potential surface and predominantly populated in the molecular beam. The differences between experimental and theoretical frequencies are $< 4\ cm^{-1}$, which is of the order of the experimental resolution. The bands A–F in the $C_6H_5^+\cdot Ar_2$ spectrum are assigned to a c-$C_6H_5^+\cdot Ar_2(\sigma,\pi)$ trimer, in which a π-bonded Ar atom is weakly attached to the more strongly bound c-$C_6H_5^+\cdot Ar(\sigma)$ dimer. There are essentially no changes in the IRPD spectrum, as predicted by the calculations. The good agreement between experimental and theoretical spectra confirms the previous conclusion that the ground electronic state of $C_6H_5^+$ is $^1A_1$ and not $^3B_1$ (see Figure S1 in Supporting Information).[7] The IR spectrum of c-$C_6H_5^+$ in an Ar matrix shows a single band at $3110\ cm^{-1}$ (indicated by an arrow in Figure 2), which was assigned to the intense ν_{19} mode.[7] Comparison with ν_{19} calculated for c-$C_6H_5^+$ ($3103\ cm^{-1}$) and that measured for c-$C_6H_5^+\cdot Ar_n$ ($3110 \pm 1\ cm^{-1}$) suggests that the matrix shift is small and essentially due to the first σ-bonded Ar ligand. Bands X–Z in the IRPD spectra are clearly not due to clusters with c-$C_6H_5^+$. Although an assignment to one specific of the many low-lying a-$C_6H_5^+$ isomers[12,22] is presently impossible,[23] the IRPD spectra in Figure 2 provide the first spectroscopic evidence for efficient ring opening of halobenzenes upon electron ionization.

Comparison of the C–H bond properties of c-$C_6H_5^+$ with those of the phenyl radical[24] establishes the effects of ionization on the C–H bond strength. The σ_{CH} frequencies of c-C_6H_5 are 3086 (ν_1), 3072 (ν_2), 3037 (ν_3), 3071 (ν_{19}), and 3060 (ν_{20}) cm^{-1}. Thus, all σ_{CH} frequencies in c-C_6H_5 (except ν_3) are ca. $20\ cm^{-1}$ lower than those measured for c-$C_6H_5^+\cdot Ar_n$, confirming the predicted ionization-induced contraction of the C–H bonds.[6b]

The angle θ of the phenyl ring is a sensitive structural indicator for the type of bonding of c-$C_6H_5^+$ to ligands (Table 3).[8,13,16] It decreases from $\theta = 150°$ for isolated c-$C_6H_5^+$ in [c-$C_6H_5\cdot L]^+$ in the order L = Ar (140°), HF (134°), N_2 (125°), and CO (124°) as a result of increasing electron transfer from L to c-$C_6H_5^+$. This trend correlates with the rising [c-$C_6H_5\cdot L]^+$ dissociation energies ($D_0 = 13.4$–$297\ kJ\,mol^{-1}$) and the contraction of the corresponding bonds (R_{C_1L} = 2.17–1.39 Å). Apparently, this geometrical change is also reflected in the *ortho* C–H bond length, R_{C_2H}, and the corresponding frequency of ν_{19}. These predicted trends are confirmed by available experimental IR spectra of [c-$C_6H_5\cdot L]^+$.[8,16]

In conclusion, Ar-tagging IRPD spectroscopy provides the first spectroscopic and structural characterization of c-$C_6H_5^+$ in the gas phase. The analysis of σ_{CH} frequencies unravels details of C–H bond properties in this fundamental aryl cation. The interaction with Ar is a sensitive probe for the electrophilicity of the vacant nonbonding σ orbital of c-$C_6H_5^+$. Finally, IRPD spectra of $C_6H_5^+\cdot Ar_n$ demonstrate spectroscopically for the first time that electron impact of halobenzene molecules produces substantial fractions of a-$C_6H_5^+$ ions, whereas ring-opening processes are largely suppressed using softer photolysis and photoionization techniques.

Table 3: Selected structural, vibrational, and energetic parameters of selected [c-$C_6H_5\cdot L]^+$ ions evaluated at the MP2/6-311++G(2df,2pd) level.[a]

[c-$C_6H_5\cdot L]^+$	D_0 [kJ mol^{-1}]	θ [°]	R_{C_1L} [Å]	ν_{19} [cm^{-1}]	ν_s [cm^{-1}]	R_{C_2H} [Å]	$q_{C_6H_5}$ [e]
c-$C_6H_5^+$	–	149.7	–	3103	–	1.0784	+1.0
[c-$C_6H_5\cdot Ar]^+$	13.4	139.7	2.1798	3110	93	1.0775	+0.75
[c-$C_6H_5\cdot FH]^+$	54.2	133.7	1.6181	3099	360	1.0787	+0.73
[c-$C_6H_5\cdot N_2]^+$	141.6	125.4	1.3850	3074	1120	1.0808	+0.51
[c-$C_6H_5\cdot CO]^+$	297.3	123.6	1.3892	3071	1218	1.0809	+0.27

[a] Harmonic frequencies are scaled by 0.9469.[16a]

Experimental and Theoretical Methods

IRPD spectra of $C_6H_5^+\cdot Ar_n$ clusters were recorded in a tandem quadrupole mass spectrometer (QMS1/2).[18,19] $C_6H_5^+\cdot Ar_n$ were generated in a pulsed supersonic molecular beam expansion by chemical ionization of two different gas mixtures. Electron ionization (EI) of fluorobenzene seeded in 8 bar Ar resulted in the formation of $C_6H_5^+$ ions through facile F atom elimination, and $C_6H_5^+\cdot Ar_n$ were generated by subsequent three-body aggregation. In addition to c-$C_6H_5^+$, this procedure produced substantial concentrations of less stable a-$C_6H_5^+$ isomers, due to significant excess energy available in the EI process of fluorobenzene.[25] In contrast, EI of benzaldehyde seeded in 5 bar Ar generated $C_6H_5^+$ by sequential elimination of H and CO. As a result of this more energy-demanding two-step process, mainly c-$C_6H_5^+$ ions are formed, because less energy is available to overcome the barrier for ring opening required for the generation of a-$C_6H_5^+$ isomers. $C_6H_5^+\cdot Ar_n$ ions were mass selected by QMS1 and irradiated in an octopole with a tunable IR laser pulse (ν_{IR}). Resonant vibrational excitation of $C_6H_5^+\cdot Ar_n$ induced the rupture of the weak intermolecular bonds [Eq. (1)]:

$$C_6H_5^+ \cdot Ar_n + h\nu_{IR} \rightarrow C_6H_5^+ + n\,Ar \quad (1)$$

$C_6H_5^+$ fragment ions were selected by QMS2 and monitored as a function of ν_{IR} to obtain IRPD spectra of $C_6H_5^+\cdot Ar_n$. Ab initio calculations were carried out at the MP2/aug-cc-pVTZ level.[26] Binding energies were corrected for zero-point vibrational energies and basis set superposition error. Harmonic vibrational wavenumbers were scaled by 0.951. The charge distribution was evaluated using the natural bond orbital population analysis.

Received: October 10, 2010
Published online: November 29, 2010

Keywords: carbocations · IR spectroscopy · phenyl cation · structure elucidation

[1] a) T. Snow, L. V. Page, Y. Keheyan, V. M. Bierbaum, *Nature* **1998**, *391*, 259; b) C. N. Keller, V. G. Anicich, T. E. Cravens, *Planet. Space Sci.* **1998**, *46*, 1157; c) D. Smith, *Chem. Rev.* **1992**, *92*, 1473.

[2] P. J. Linstrom, W. G. Mallard, NIST Chemistry WebBook, NIST Standards and Technology, Gaithersburg MD, 20899 (http://webbook.nist.gov), **2001**.

[3] N. Solcà, O. Dopfer, *Angew. Chem.* **2002**, *114*, 3781; *Angew. Chem. Int. Ed.* **2002**, *41*, 3628.
[4] H. S. Andrei, N. Solca, O. Dopfer, *Angew. Chem.* **2008**, *120*, 401; *Angew. Chem. Int. Ed.* **2008**, *47*, 395.
[5] O. Dopfer, D. Roth, J. P. Maier, *J. Am. Chem. Soc.* **2002**, *124*, 494.
[6] a) A. Nicolaides, D. M. Smith, F. Jensen, L. Radom, *J. Am. Chem. Soc.* **1997**, *119*, 8083; b) J. Hrusak, D. Schröder, S. Iwata, *J. Chem. Phys.* **1997**, *106*, 7541.
[7] M. Winkler, W. Sander, *Angew. Chem.* **2000**, *112*, 2091; *Angew. Chem. Int. Ed.* **2000**, *39*, 2014.
[8] N. Solcà, O. Dopfer, *J. Am. Chem. Soc.* **2003**, *125*, 1421.
[9] a) H. Zollinger, *Angew. Chem.* **1978**, *90*, 151; *Angew. Chem. Int. Ed. Engl.* **1978**, *17*, 141; b) R. G. Bergstrom, R. G. M. Landells, G. H. Wahl, H. Zollinger, *J. Am. Chem. Soc.* **1976**, *98*, 3301.
[10] a) V. Butcher, M. L. Costa, J. M. Dyke, A. R. Ellis, A. Morris, *Chem. Phys.* **1987**, *115*, 261; b) N. E. Sveum, S. J. Goncher, D. M. Neumark, *Phys. Chem. Chem. Phys.* **2006**, *8*, 592.
[11] a) M. Speranza, *Chem. Rev.* **1993**, *93*, 2933; b) M. Speranza, Y. Keheyan, G. Angelini, *J. Am. Chem. Soc.* **1983**, *105*, 6377; c) S. Fornarini, M. Speranza, *J. Am. Chem. Soc.* **1985**, *107*, 5358; d) G. Angelini, S. Fornarini, M. Speranza, *J. Am. Chem. Soc.* **1982**, *104*, 4773.
[12] a) P. Ausloos, S. G. Lias, T. J. Buckley, E. E. Rogers, *Int. J. Mass Spectrom. Ion Process.* **1989**, *92*, 65; b) J. C. Lorquet, A. J. Lorquet, *J. Phys. Chem. A* **2001**, *105*, 3719.
[13] Y. A. Ranasinghe, G. L. Glish, *J. Am. Soc. Mass Spectrom.* **1996**, *7*, 473.
[14] E. J. Bieske, O. Dopfer, *Chem. Rev.* **2000**, *100*, 3963.
[15] O. Dopfer, R. V. Olkhov, J. P. Maier, *J. Chem. Phys.* **1999**, *111*, 10754.
[16] a) A. Patzer, S. Chakraborty, O. Dopfer, *Phys. Chem. Chem. Phys.* **2010**, DOI: 10.1039/c0cp00696c; b) M. Winkler, W. Sander, *J. Org. Chem.* **2006**, *71*, 6357.
[17] a) K. Hiraoka, I. Kudaka, S. Yamabe, *Chem. Phys. Lett.* **1991**, *178*, 103; b) R. V. Olkhov, S. A. Nizkorodov, O. Dopfer, *J. Chem. Phys.* **1998**, *108*, 10046.
[18] O. Dopfer, *Int. Rev. Phys. Chem.* **2003**, *22*, 437.
[19] O. Dopfer, *Z. Phys. Chem.* **2005**, *219*, 125.
[20] a) N. Solcà, O. Dopfer, *Chem. Eur. J.* **2003**, *9*, 3154; b) H. J. Neusser, K. Siglow, *Chem. Rev.* **2000**, *100*, 3921.
[21] These planar structures feature bifurcated hydrogen bonds to two adjacent C–H protons of c-$C_6H_5^+$. These weak bonds have essentially no impact on the geometric, electronic, and vibrational properties of c-$C_6H_5^+$.
[22] M. Tasaka, M. Ogata, H. Ichikawa, *J. Am. Chem. Soc.* **1981**, *103*, 1885.
[23] Band X at 2970 falls in the range of aliphatic C–H stretch modes, whereas bands Y and Z at 3200 and 3276 cm^{-1} are typical for acetylenic C–H stretch modes of carbocations.[3,5,27]
[24] a) E. N. Sharp, M. A. Roberts, D. J. Nesbitt, *Phys. Chem. Chem. Phys.* **2008**, *10*, 6592; b) A. V. Friderichsen, J. G. Radziszewski, M. R. Nimlos, P. R. Winter, D. C. Dayton, D. E. David, G. B. Ellison, *J. Am. Chem. Soc.* **2001**, *123*, 1977; c) A. Lapinski, J. Spanget-Larsen, M. Langgard, J. Waluk, J. G. Radziszewski, *J. Phys. Chem. A* **2001**, *105*, 10520.
[25] Similar results were obtained with bromobenzene.
[26] M. J. Frisch et al., Gaussian 03, Revision C.02., Gaussian, Inc, Pittsburgh PA **2004**.
[27] O. Dopfer, R. V. Olkhov, M. Mladenovic, P. Botschwina, *J. Chem. Phys.* **2004**, *121*, 1744.

